A study of 1D inversion of EM34 data from 3D media

Gabriel Pinto Santos (UFPA) and Cícero Régis (UFPA, INCT-GP)

Abstract

This study presents an example of 1D inversion of synthetic 3D data from horizontal and vertical magnetic dipoles, focusing on the configurations used in the EM34 equipment. The inversion code is an implementation of the Gauss-Newton method with Levenberg-Marquardt iterations, with the inclusion of smoothness constraints to the model parameters. The 1D inversion generates a layered model for each measurement point in an EM34 survey. The synthetic data is from a 3D model composed of a two-layer background with a 3D conductive block close to the surface. The results indicate a minimum distance from the 3D conductive body for which its influence on the responses is small enough to make the 1D inversion feasible. Also, the study illustrates the insurmountable unsuitability of applying 1D inversion to data acquired over truly three-dimensional geo-electrical structures.

Introduction

Near surface electromagnetic surveys are routinely performed for a large number of applications, including mineral and ground water exploration, environmental monitoring, archaeological studies and many more. In the past, interpretation was only performed directly from the acquired data, either in the form of electromagnetic field components or apparent resistivities. Today, the available computer resources (hardware and software) allow for the application of inversion methods that usually yield better data for a more accurate interpretation.

Performing inversion of three-dimensional electromagnetic data is a highly costly computational task. Therefore, it is a common practice to invert data using 1D layered models, which is a fast process that may generate accurate results if the geological environment from which the data were acquired is at least approximately one-dimensional. However, in true three-dimensional cases, a quick 1D inversion simply can not be applied, for it will generate meaningless solutions.

This paper shows an illustration of these problems by 1D inverting synthetic electromagnetic data generated from a simple 3D model. For this example, we have modeled data from horizontal and vertical magnetic dipoles, as used in the Slingram method, with a focus on the EM34 equipment.

The inversion code is an implementation of the Gauss-Newton method with Levenberg-Marquardt iterations (Gómez-Treviño et al., 2002; Pujol, 2007) and the inclusion of smoothness constraints (Constable et al., 1987) to the model parameters, which in this case are the layer resistivities.

The results indicate that fast 1D solutions must be used with caution and that the geophysicist must be able to recognize the instances when they are truly useful.

Methodology

The Slingram method used in the EM-34 equipment allows for the estimation of electrical conductivity in subsurface through measurements of the secondary magnetic field variation (McNeill, 1980). It operates by measuring the electromagnetic field in the frequency domain and its interactions with the lithological medium. The equipment consists of two coils: the first one is energized by an alternating current and is responsible for generating the primary electromagnetic field, which in turn induces current in the subsurface, producing a secondary electromagnetic field. The second coil acts as the receiver, positioned at fixed distances from the transmitter in pre-determined configurations.

In the coplanar configurations used by the EM34 equipment, the horizontal ($\mathbf{H}_y$) and vertical ($\mathbf{H}_z$) components of the magnetic fields are generated by, respectively, the horizontal (HMD) and vertical (VMD) magnetic dipole sources.

Forward modeling

For the layered (1D) problem, the calculation of the fields in the receiver position requires the numerical evaluation of improper integrals of the Hankel transform (Ward & Hohmann, 1988, pp. 208 and 223). The 1D solutions are used in the calculation of the magnetic field in the forward 1D problem and also to calculate the electric field from the sources to be used as primary field in the 3D formulation. For the VMD the integrals are evaluated using the digital filter presented by Werthmüller et al. (2019) and for the HMD using the method of Quadrature With Extrapolation (Key, 2012).

The three-dimensional modeling program is an implementation of the Vector Finite Element method, as described by Jin (2015), with a secondary field formulation to calculate directly the magnetic field. The finite element 3D mesh is built with the TETGEN mesh generator (**?**). The method generates a very large and sparse linear system

of equations that is solved using the PARDISO software (Schenk et al., 2001).

1D inversion

Given the field observations contained in the vector **y**, the objective of the inversion is to determine the values of a parameter vector **p** that generate synthetic data that best fit the observations. In this case, the observed data are the apparent conductivities or the imaginary component of the magnetic field and the model parameters are the layer resistivities in the model.

The functional to be minimized $\Phi(\mathbf{p})$ is defined as:

$$\Phi(\mathbf{p}) = \phi^d(\mathbf{p}) + \alpha\ \phi^v(\mathbf{p}), \tag{1}$$

where

$$\phi^d(\mathbf{p}) = \frac{1}{2}\sum_{i=1}^{m}[\mathbf{y}_i^0 - f_i(x_i,\mathbf{p})]^2 \tag{2}$$

is the functional that represents the fitting of the observations by the data generated by the mathematical model f, which depends on **p** and independent variables such as frequency and measurement positions. The constraint function

$$\phi^v(\mathbf{p}) = \frac{1}{2}(\mathbf{p}_1 - \mathbf{p}_2)^2 + (\mathbf{p}_2 - \mathbf{p}_3)^2 + \cdots + (\mathbf{p}_{n-1} - \mathbf{p}_n)^2] \tag{3}$$

defines *a priory* equality relationships between adjacent parameters to impose smoothness in the solution. In the objective function (1), α is a positive scalar, known as the regularization parameter, whose function is to weigh the relative importance of the information provided by the constraint relations.

The Gauss-Newton method defines the sensitivity matrix **A**, whose elements are

$$\mathbf{A} = \frac{\partial \phi_i^d}{\partial p_j} = -\sum_{i=1}^{m}[\mathbf{y}_i^0 - f_i(x_i,p_j)]\frac{\partial \phi_i^d}{\partial p_j}, \tag{4}$$

and the residual vector

$$\delta\mathbf{y}_i = \mathbf{y}_i^0 - f_i(x_i,\mathbf{p}_j). \tag{5}$$

Then the method produces an estimate of **p** that minimizes the objective function (eq. 1) by iterating the equation

$$(\mathbf{A}^T\mathbf{A} + \alpha\mathbf{M}^T\mathbf{M})\delta\mathbf{p}_k = \mathbf{A}^T\delta\mathbf{y} + \alpha\mathbf{M}^T\mathbf{M}\mathbf{p}, \tag{6}$$

The relationships between parameters that define the constraint function (eq. 3) are expressed in the matrix **M** as

$$\mathbf{M} = \begin{bmatrix} 1 & -1 & 0 & \dots & 0 & 0 \\ 0 & 1 & -1 & \dots & 0 & 0 \\ 0 & 0 & 1 & \dots & 0 & 0 \\ & & \vdots & & & \\ 0 & 0 & 0 & \dots & 1 & -1 \end{bmatrix}, \tag{7}$$

which leads to the square matrix

$$\mathbf{M}^T\mathbf{M} = \begin{bmatrix} 1 & -1 & 0 & \dots & 0 & 0 \\ -1 & 2 & -1 & \dots & 0 & 0 \\ 0 & -1 & 2 & \dots & 0 & 0 \\ & & \vdots & & & \vdots \\ 0 & 0 & 0 & \dots & 2 & -1 \\ 0 & 0 & 0 & \dots & -1 & 1 \end{bmatrix} \tag{8}$$

The Marquardt technique aims to ensure that the convergence estimate always takes a step in the descending direction of the gradient. This is achieved by alternating between an estimate using the Gauss-Newton method and taking a small step in the descending direction of the gradient. Combining the two kinds of steps for minimizing the fitting functional into a single equation is achieved by adding a positive scalar λ, called the Marquardt parameter, to the diagonal of the Hessian matrix of the functionals, so that the iteration becomes

$$(\mathbf{A}^T\mathbf{A} + \alpha\mathbf{M}^T\mathbf{M} + \lambda I), \delta\mathbf{p}_k = \mathbf{A}^T\delta\mathbf{y} + \alpha\mathbf{M}^T\mathbf{M}\mathbf{p}, \tag{9}$$

The value of λ is decreased in an iteration if the value of the objective function Φ decreases. Otherwise, its value is increased and a new $\delta\mathbf{p}$ is generated. This step is repeated until Φ decreases in the iteration.

The iteration of equation 9 is repeated until the objective function reaches a minimum or a maximum number of iterations is reached, which signifies that the process didn't converge.

Results and discussions

The model is composed of only two layers. The first layer has a resistivity of 50 Ω m and a thickness of 30 meters, and the second layer is an infinite basement with a resistivity of 500 Ω m. Embedded in the first layer, at a 2 m depth, is a conductive (10 Ωm) cube with a 10 m edge. A schematic example of the model is shown in figure 1.

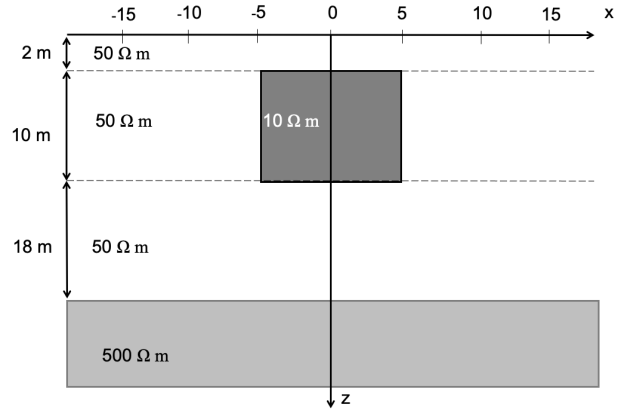

Figure 1: 3D model that generated the synthetic data.

The synthetic data were generated simulating the three configurations of the EM34 equipment, with three

measurements at each point for the HMD and the VMD coplanar configurations, using three offset/frequency pairs: 10 m at 6.4 kHz; 20 m at 1.6 kHz; and 40 m at 400 Hz. Data were generated at 200 positions, distributed along a profile ranging from -500 m to 500 m.

This study performed the joint inversion of synthetic data from both the HMD and the VMD at the same measurement positions. The 1D inversion was performed using the regularization parameter $\alpha = 10^{-9}$. The interpretive model has only 7 layers with varying thicknesses.

At positions far from the 3D block the inversion is able to fit the data, because the influence of the block is small. To illustrate this behavior, figure 2 shows that at 500 m from the block the inversion is able to capture the values of both layers by closely fitting the data.

At positions above the block, on the other hand, it is impossible for the 1D inversion to find an adequate fitting. Figure 3 shows the results for the position exactly above the center of the block. In this case, the inversion can not converge because the data from a layered model can not reproduce those which are under the influence of the 3D body. This means that the layer resistivities produced at the end of the (non converging) process are meaningless and must not be interpreted in any way.

The results from all 200 points are shown in figure 4 for all 6 configurations. These plots show the measured magnetic component at each point, comparing the original data with those resulting from the inverted layered models. It is clear that only at distances over at least twice the offsets there is an adequate fit between the curves.

A final illustration comes from building the resistivity section from the models generated by the inversion. The lateral borders of the section in figure 5 reproduce the layered model, but the structure observed in the central part has no correspondence whatsoever to the true model that generated the data.

Conclusions

The results are an indication the limits of applying one-dimensional inversion to problems that require more complex and expensive solutions. They are just exactly what is expected (1D solutions are good for 1D environments and bad otherwise), but this is an illustration of a situation that often arises in the practice of electromagnetic geophysical methods.

This study is meant as a cautionary note to those who work with near surface electromagnetic data and need to go beyond interpreting apparent conductivities: 1D inversion is fast and cheap, but do not trust its results blindly, under penalty of ending with interpretations that have no relation to the actual geology of your study area.

Acknowledgements

The authors thank Petrobras for the support to this research through project number 2017/00424-6.

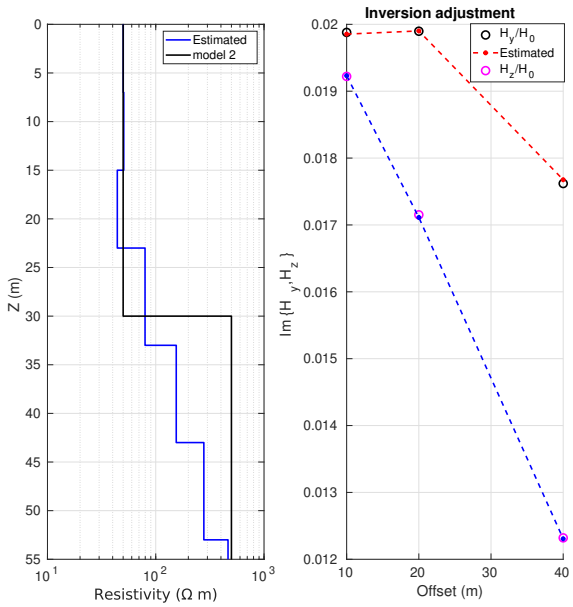

Figure 2: Inversion results at 500 m from the 3D block. Left: Layered models; Right: Data fit.

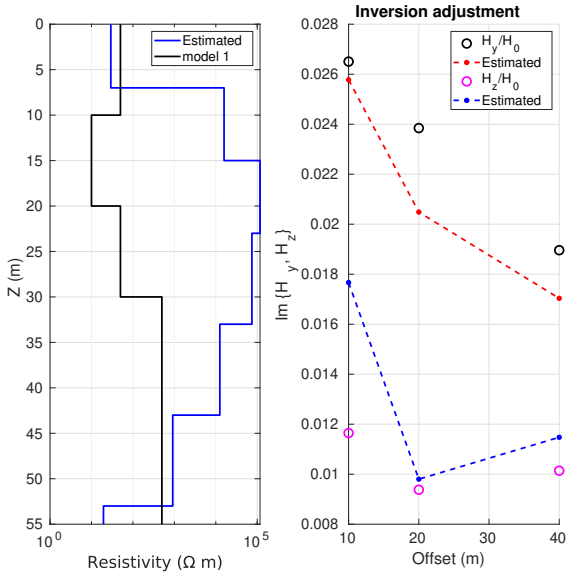

Figure 3: Inversion results above the center of the 3D block. Left: Layered models; Right: Data fit.

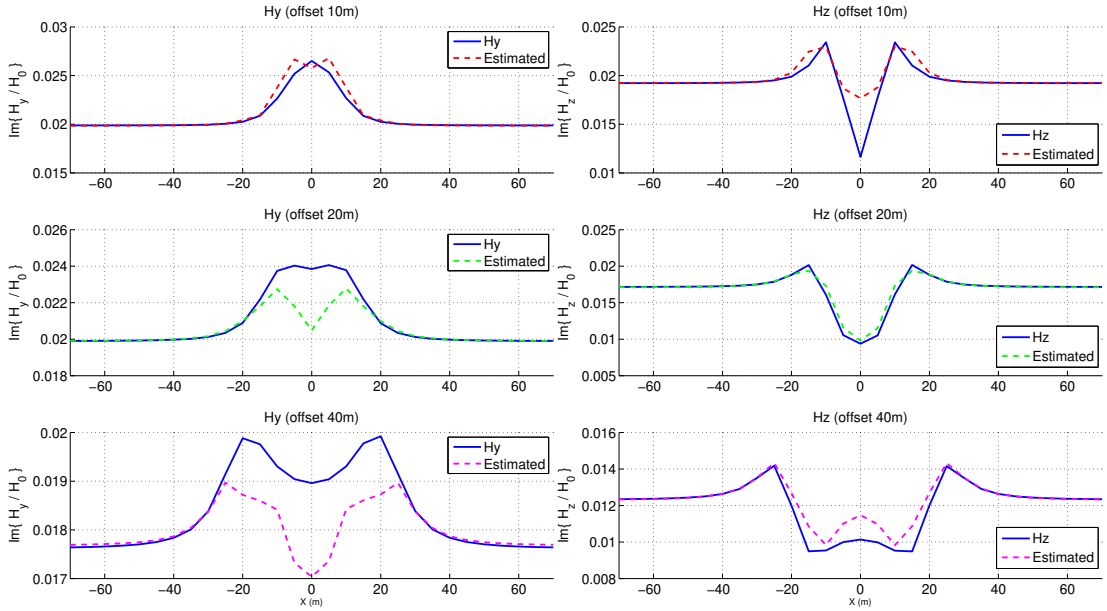

Figure 4: Comparison between the original data and those generated by the 1D inversion.

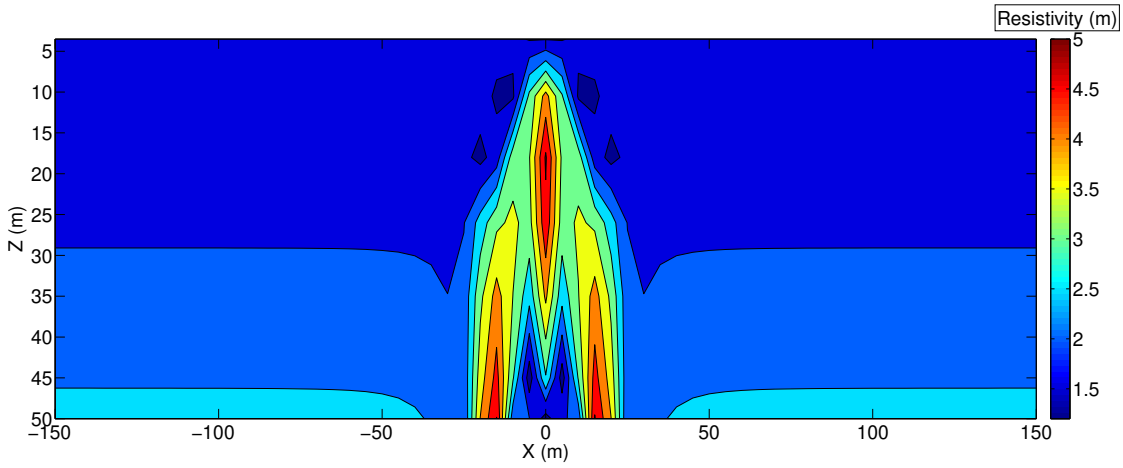

Figure 5: Resistivities from the inverted layered models.

References

Constable, S. C., Parker, R. L. & Constable, C. G., 1987. Occam's inversion: a practical algorithm for generating smooth models from em sounding data, Geophysics, vol. 52(3): 289–300.

Gómez-Treviño, E., Esparza, F. J. & Méndez-Delgado, S., 2002. New theoretical and practical aspects of electromagnetic soundings at low induction numbers, Geophysics, vol. 67(5): 1441–1451.

Jin, J.-M., 2015. The Finite Element Method in Electromagnetics, 3rd ed., Wiley.

Key, K., 2012. Is the fast hankel transform faster than quadrature?, Geophysics, vol. 77(3): F21–F30.

McNeill, J. D., 1980. Electromagnetic terrain conductivity measurements at low induction numbers, Technical Note TN-6, Geonics Ltd.

Pujol, J., 2007. The solution of nonlinear inverse problems and the Levenberg-Marquardt method, Geophysics, vol. 72(4): W1–W16, doi:10.1190/1.2732552.

Schenk, O., Gärtner, K., Fichtner, W. & Stricker, A., 2001. Pardiso: a high-performance serial and parallel sparse linear solver in semiconductor device simulation, Future Generation Computer Systems, vol. 18(1): 69 – 78, doi:https://doi.org/10.1016/S0167-739X(00)00076-5, i. High Performance Numerical Methods and Applications. II. Performance Data Mining: Automated Diagnosis, Adaption, and Optimization.

Ward, S. H. & Hohmann, G. W., 1988. Electromagnetic theory for geophysical applications, in: Electromagnetic Methods in Applied Geophysics: Voume 1, Theory, Society of Exploration Geophysicists, 130–311.

Werthmüller, D., Key, K. & Slob, E. C., 2019. A tool for designing digital filters for the hankel and fourier transforms in potential, diffusive, and wavefield modeling, GEOPHYSICS, vol. 84(2): F47–F56, doi: 10.1190/geo2018-0069.1.